Mono-[^{123}I]Iodohypericin

[^{123}I]MIH

Arvind Chopra, PhD[1]

Created: February 6, 2008; Updated: March 12, 2008.

Chemical name:	Mono-[^{123}I]Iodohypericin
Abbreviated name:	[^{123}I]MIH
Synonym:	
Agent Category:	Compound
Target:	Necrotic tissue
Target Category:	Uptake
Method of detection:	Single-photon emission computed tomography (SPECT) or gamma planar imaging
Source of signal:	^{123}I
Activation:	No
Studies:	• Rodents • Non-primate non-rodent mammals

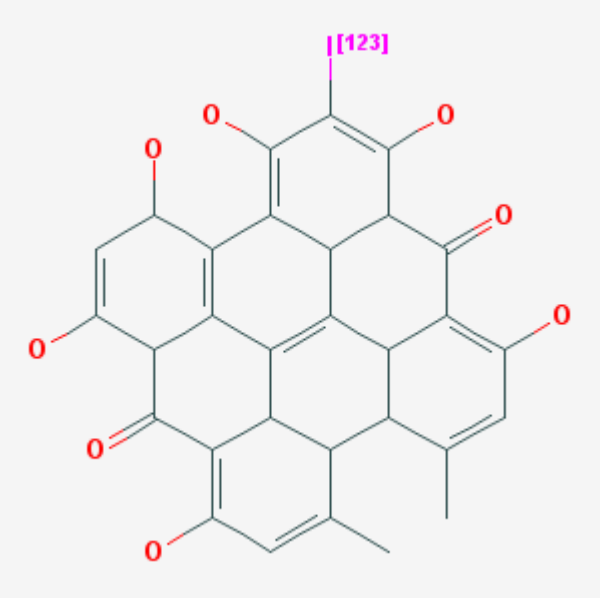

Click on the above structure for additional information in PubChem.

Background

[PubMed]

[1] National Center for Biotechnology Information, NLM, NIH, Bethesda, MD 20894; Email: micad@ncbi.nlm.gov.

NLM Citation: Chopra A. Mono-[^{123}I]Iodohypericin. 2008 Feb 6 [Updated 2008 Mar 12]. In: Molecular Imaging and Contrast Agent Database (MICAD) [Internet]. Bethesda (MD): National Center for Biotechnology Information (US); 2004-2013.

Approximately 2% of patients suffering from acute myocardial infarction (AMI) may be typically misdiagnosed on the basis of the presence of a characteristic chest pain or an altered electrocardiogram or biomarker pattern. Although this is only a small percentage of the total number of patients, the number of misdiagnosed AMI incidents is in the thousands because the total number of individuals suffering from AMI is very large (more than one million in the United States alone) (1). A quick diagnosis of AMI is important to devise a suitable treatment and increase the chances of a favorable outcome. The use of scintigraphic agents such as pyrophosphate labeled with radioactive technetium (^{99m}Tc), which targets the calcium phosphate deposit in the myocardial tissue, or the F(ab) fragment of an anti-myosin antibody (labeled with radioactive indium), or [^{99m}Tc]glucarate has been attempted for the diagnosis of AMI, but all these agents have some limitations (2). The pyrophosphate shows a low affinity and specificity for the necrotic myocardium in AMI patients, and the antibody is no longer available commercially (2). Although [^{99m}Tc]glucarate appears to be a promising agent for the detection and quantification of infarct AMI, it is rapidly washed out from the infarcted myocardium; thus, a meaningful scan can be obtained only for a short time (<9 h) after the infarct has occurred because in the necrotic tissue it targets positively charged histones, which disintegrate rapidly (2). Myocardial perfusion imaging is also performed with other radiopharmaceuticals using either positron-emission tomography (PET) or single-photon emission computed tomography (SPECT), but all these agents have limitations as described in detail by Cuocolo et al. (3).

Hypericin, a polycyclic polyaromatic quinone found in the Saint John's wort plant (*Hypericum perforatum*), was shown to possess antiviral and antineoplastic characteristics (4). This compound has a chemical structure that is similar to some porphyrin derivatives that were shown to be photosensitizers that specifically targeted the necrotic tissue in neoplastic tumors and could be used for photodynamic therapy of cancer (5). Because porphyrins bound primarily to the necrotic tissue, they were also used by investigators as magnetic resonance imaging contrast agents to visualize AMI under preclinical conditions (6, 7). Bearing this in mind, investigators have evaluated the use of hypericin for the detection and imaging of necrotic tissue, including that which results from AMI (8-11). To achieve this, hypericin was derivatized with radioactive iodine (^{123}I) to obtain mono-[^{123}I]iodohypericin ([^{123}I]MIH) and then used for SPECT imaging studies (8-11).

Synthesis

[PubMed]

The synthesis of hypericin from emodin was patented and described elsewhere by Mazur et al. (12).

Hypericin was radioiodinated using an electrophilic substitution reaction with sodium [^{123}I]iodide ([^{123}I]Na) (11). Briefly, hypericin in ethanol, phosphoric acid, and peracetic acid were successively added to [^{123}I]Na in sodium hydroxide. The mixture was incubated for 30 min at room temperature, and the reaction products were purified with reverse-

phase high-performance liquid chromatography on a reverse-phase C_{18} column. The fractions containing [^{123}I]MIH were concentrated under a flow of nitrogen at 45°C. The reaction yield was reported to be 70 to 97% relative to the starting ^{123}I activity. The specific activity of [^{123}I]MIH was reported to be >25 Ci/μmol (>925 GBq/μmol) with a purity of >99% up to 24 h after formulation. The final formulation was not described in this publication (11). However, in other publications [^{123}I]MIH was reported to be formulated in 20% polyethylene glycol-400 immediately before administration (8, 9).

In one study, the biological activities of [^{123}I]MIH and it precursor, mono-[^{123}I]iodoprotohypericin ([^{123}I]MIprotoH) were compared (see below in Rodent section under Animal Studies) (9). The synthesis of [^{123}I]MIprotoH was described by Fonge et al. (9).

In Vitro Studies: Testing in Cells and Tissues

[PubMed]

No references are currently available.

Animal Studies

Rodents

[PubMed]

A preliminary biodistribution study of [^{123}I]MIH was performed by Vanbilloen et al. in mice bearing a radiation-induced fibrosarcoma tumor (13). The clearance of [^{123}I]MIH from the blood was reported to be slow and primarily *via* the hepatobiliary route. Although the uptake of [^{123}I]MIH was initially high in the lungs, it decreased gradually from 32.5% of the injected dose/g tissue (% ID/g) at 10 min to 16.2% ID/g at 24 h. During the same time period there was a gradual increase of [^{123}I]MIH accumulation in the tumor, which reached a peak of 21.3% ID/g. From these results the investigators concluded that [^{123}I]MIH was probably accumulating in the tumors because it bound to the necrosed part of the tumor. This observation prompted them to evaluate the use of this radiochemical for the detection of necrotic tissue in other organs of the body.

In another study, NMRI mice were injected with [^{123}I]MIH and killed at various time points ranging from 10 min to 24 h (n = 3 animals per time point) after administration of the radiochemical (11). The various organs and body parts were collected, and the accumulated radioactivity was counted. Approximately 30% of the injected dose was still present in the blood at 4 h after injection, probably because hypericin is lipophilic and binds to both high- and low-density lipoproteins in plasma (14). The investigators observed that 70% ID was excreted with the feces after 24 h, and <10% ID was excreted in the urine; almost no uptake was observed in the brain (11). The investigators also noted that imaging with [^{123}I]MIH was possible only 12 h after administration because they

had to allow the blood concentration of the radiochemical to drop to a suitable level for imaging.

Ni et al. evaluated the use of [^{123}I]MIH for the detection of necrosis in the rat liver (8). Images were obtained from normal (control) rats and rats with reperfused hepatic infarction 24 and 48 h after [^{123}I]MIH injection. The accumulation of radioactivity was observed only in the necrotic part of reperfused hepatic infarction animal livers that had 3.1% ID/g *versus* 0.38% ID/g in the normal liver lobes. Presence of necrosis in the liver lobes showing a high accumulation of [^{123}I]MIH was confirmed with histochemical staining (8).

The tumor-seeking properties of [^{123}I]MIH and [^{123}I]MIprotoH, a precursor of [^{123}I]MIH, were compared using a radiation-induced fibrosarcoma mouse model (9). Both radiochemicals were reported to clear rapidly from all organs and accumulated to a similar extent ($P > 0.05$) in the tumors. The clearance of [^{123}I]MIH from the blood and liver was faster than [^{123}I]MIprotoH. In addition, the tumor/blood, tumor/liver, and tumor/spleen+pancreas ratios were higher for [^{123}I]MIH than for [^{123}I]MIprotoH 24 h after administration (5.4, 1.5, and 1.7, respectively, *versus* 0.4, 0.1, and 0.1, respectively). This indicated that, compared to its precursor molecule, [^{123}I]MIH was a superior tracer for imaging tumors (9).

Other Non-Primate Mammals

[PubMed]

The use of [^{123}I]MIH for imaging necrotic tissue in the myocardium as a result of AMI was investigated in a rabbit model (8, 10). A single New Zealand rabbit with occlusive myocardial infarction was injected with [^{123}I]MIH and imaged 24 and 48 h after injection (8). Whole-body SPECT consistently showed a single spot in the anatomical area of the heart at both time points. The SPECT images also detected low levels of radioactivity in the thyroid and the intestines of the injected animals. *Ex vivo* histochemical staining and autoradiography of the myocardium confirmed that the radioactivity observed in the heart was indeed only in the infarcted regions.

In another study, Fonge et al. evaluated the use of [^{123}I]MIH for the detection and quantification of AMI in a rabbit model and compared it with the use of radioactive [^{13}N]ammonia ([^{13}N]NH_3) for the same purpose (10). Rabbits with an occluded left circumflex coronary artery (LCx) were divided into four groups. In group A ($n = 3$ animals), the artery was permanently occluded; in groups B ($n = 3$) and C ($n = 6$), the artery was reperfused by releasing the occlusion after 15 and 90 min, respectively; group D ($n = 2$) served as the control group in that the artery was not occluded at all. The animals were imaged with PET using [^{13}N]NH_3 18 h after induction of the infarct followed by an injection of [^{123}I]MIH for SPECT imaging at different time points. The animals were then killed, and the excised hearts were sliced for autoradiography and histochemical staining. In the control animals (group D), [^{13}N]NH_3 was evenly distributed throughout the left ventricular wall, but the other animals with LCx (groups A,

B, and C) showed left-ventricular perfusion defects to different degrees depending on the infarct size. The infarcts were clearly visible with SPECT imaging only 9 h after and for up to 24 h after the injection of [^{123}I]MIH. The investigators reported a perfect match between the PET and SPECT images. Autoradiography revealed that only the rabbits in group C had a strong uptake of [^{123}I]MIH, and animals in groups A, B, and D showed a low uptake of the radiochemical. Also, on histological examination only rabbits in groups A, B, and C showed myocardial injury that correlated with the degree of necrosis induced by occlusion of the LCx.

Non-Human Primates

[PubMed]

No references are currently available.

Human Studies

[PubMed]

No references are currently available.

Supplemental Information

[Disclaimers]

References

1. Pope J.H., Aufderheide T.P., Ruthazer R., Woolard R.H., Feldman J.A., Beshansky J.R., Griffith J.L., Selker H.P. Missed diagnoses of acute cardiac ischemia in the emergency department. N Engl J Med. 2000;342(16):1163–70. PubMed PMID: 10770981.
2. Flotats A., Carrio I. Non-invasive in vivo imaging of myocardial apoptosis and necrosis. Eur J Nucl Med Mol Imaging. 2003;30(4):615–30. PubMed PMID: 12638039.
3. Cuocolo A., Acampa W., Imbriaco M., De Luca N., Iovino G.L., Salvatore M. The many ways to myocardial perfusion imaging. Q J Nucl Med Mol Imaging. 2005;49(1): 4–18. PubMed PMID: 15724132.
4. Miskovsky P. Hypericin--a new antiviral and antitumor photosensitizer: mechanism of action and interaction with biological macromolecules. Curr Drug Targets. 2002;3(1):55–84. PubMed PMID: 11899265.
5. Magro C.M., Abbas A.E., Ross P. Jr. The application of photodynamic therapy in the treatment of metastatic endobronchial disease. Lasers Surg Med. 2006;38(5):376–83. PubMed PMID: 16671103.
6. Lee S.S., Goo H.W., Park S.B., Lim C.H., Gong G., Seo J.B., Lim T.H. MR imaging of reperfused myocardial infarction: comparison of necrosis-specific and intravascular contrast agents in a cat model. Radiology. 2003;226(3):739–47. PubMed PMID: 12601203.

7. Choi S.I., Choi S.H., Kim S.T., Lim K.H., Lim C.H., Gong G.Y., Kim H.Y., Weinmann H.J., Lim T.H. Irreversibly damaged myocardium at MR imaging with a necrotic tissue-specific contrast agent in a cat model. Radiology. 2000;215(3):863–8. PubMed PMID: 10831712.
8. Ni Y., Huyghe D., Verbeke K., de Witte P.A., Nuyts J., Mortelmans L., Chen F., Marchal G., Verbruggen A.M., Bormans G.M. First preclinical evaluation of mono-[123I]iodohypericin as a necrosis-avid tracer agent. Eur J Nucl Med Mol Imaging. 2006;33(5):595–601. PubMed PMID: 16450141.
9. Fonge H., Van de Putte M., Huyghe D., Bormans G., Ni Y., de Witte P., Verbruggen A. Evaluation of tumor affinity of mono-[(123)I]iodohypericin and mono-[(123)I]iodoprotohypericin in a mouse model with a RIF-1 tumor. Contrast Media Mol Imaging. 2007;2(3):113–9. PubMed PMID: 17546702.
10. Fonge H., Vunckx K., Wang H., Feng Y., Mortelmans L., Nuyts J., Bormans G., Verbruggen A., Ni Y. Non-invasive detection and quantification of acute myocardial infarction in rabbits using mono-[123I]iodohypericin {micro}SPECT. Eur Heart J. 2008;29(2):260–9. PubMed PMID: 18156139.
11. Bormans G., Huyghe D., Christiaen A., Verbeke K., de Groot T., Vanbilloen H., de Witte P., Verbruggen A. Preparation, analysis and biodistribution in mice of iodine-123 laballed derivatives of hypericin. J Label Comp Radiopharm. 2004;47:191–198.
12. Mazur, Y., H. Bock, and D. Lavie, *Preparation of hypericin.*, in *United States Patent Office*, U.S.P. Office, Editor. 1992, Yeda Research and Development Co. Ltd.: United States.
13. Vanbilloen H., Bormans G., Chen B., de Witte P., Verbruggen A., Verbeke K. Synthesis and preliminary evaluation of mono-[123I]iodohypericin. J Label Comp Radiopharm. 2001;44 Suppl. 1:S965–S967.
14. Lavie G., Mazur Y., Lavie D., Meruelo D. The chemical and biological properties of hypericin--a compound with a broad spectrum of biological activities. Med Res Rev. 1995;15(2):111–9. PubMed PMID: 7739292.